Growth and characterization of $CaCu_3Ru_4O_{12}$ single crystal*

Wang Rong-Juan(王蓉娟)[a], Zhu Yuan-Yuan(朱媛媛)[a], Wang Li(王 理)[a], Liu Yong(刘 雍)[a]†, Shi Jing(石 兢)[a]‡, Xiong Rui(熊 锐)[a], and Wang Jun-Feng(王俊峰)[b]

[a] *Key Laboratory of Artificial Micro- and Nano-structures of Ministry of Education and School of Physics and Technology, Wuhan University, Wuhan* 430072, *China*

[b] *Wuhan High Magnetic Field Center, Huazhong University of Science and Technology, Wuhan* 430074, *China*

(Received 22 April 2015; revised manuscript received 25 May 2015; published online 21 July 2015)

High-quality single crystals of A-site ordered perovskite oxides $CaCu_3Ru_4O_{12}$ were synthesized by flux method with CuO serving as a flux. The typical size of these single crystals was around $1 \times 1 \times 1$ mm^3 and the lattice constant was determined to be 7.430 ± 0.0009 Å by using x-ray single crystal diffraction. The surfaces of the samples were identified to be (100) surface. The high quality of the single crystal samples was confirmed by the rocking curve data which have a full width at half maximum of approximately 0.02 degree. The x-ray photoelectron spectroscopy measurement was performed and the temperature-dependent specific heat, magnetic susceptibility, and electric resistivity were measured along the [100] direction of the single crystals. All these measurements showed that the physical properties of $CaCu_3Ru_4O_{12}$ single crystals are similar to that of polycrystals. However, the single crystals have a lower Curie susceptibility tail and a smaller residual resistivity than polycrystals, which indicates that the amount of paramagnetic impurities can be controlled by tuning the number of defects in $CaCu_3Ru_4O_{12}$ samples.

Keywords: heavy fermion, single crystal growth, d electron oxides, perovskites

PACS: 75.30.Mb, 81.10.–h, 71.27.+a, 74.70.Pq **DOI:** 10.1088/1674-1056/24/9/097501

1. Introduction

A-site ordered perovskite oxides $AA'_3B_4O_{12}$ have attracted much scientific attention due to their significant physical properties.[1–5] By changing ions at B sites, distinct properties can be introduced to these oxides with identical crystal structure. For example, in a $CaCu_3B_4O_{12}$ system, filling B sites with Ti atoms results in a giant dielectric material with an antiferromagnetic order,[1,2] while Mn atoms at B sites lead to a giant magnetoresistance ferromagnetic material.[3,4] Moreover, different from these two oxides, $CaCu_3Ru_4O_{12}$[5] is a metal without magnetic ordering down to 50 mK, and is considered as an electrode material for $CaCu_3Ti_4O_{12}$ capacitors.[6]

Labeau *et al.*[7] first synthesized polycrystalline samples of $CaCu_3Ru_4O_{12}$ and established it to have metal-like conductivity. Subramanian *et al.*[8] claimed that the conductivity of $CaCu_3Ru_4O_{12}$ is higher than those of metallic ruthenium oxides $CaRuO_3$ and $SrRuO_3$. Furthermore, a comprehensive study of Kobayashi *et al.*[5] revealed some novel properties in this kind of ruthenium compounds: i) the electric resistivity is proportional to T^2 between 2 K and 30 K, indicating a Fermi liquid behavior; ii) the temperature-dependent magnetic susceptibility shows a Pauli metallic paramagnetic behavior, but the value of the susceptibility is higher than that of free electrons by two orders of magnitude at the room temperature. Meanwhile, a broad peak of the magnetic susceptibility exists at around 200 K; iii) the electron specific heat coefficient of $CaCu_3Ru_4O_{12}$ is 84 mJ/(mol·K^2), which is 20–30 times greater than that of free electrons. This implies an enhanced effective mass of electrons and a large density of states at the Fermi level. Moreover, it is reported that many heavy fermion systems show non-Fermi liquid (NFL) properties below a certain temperature.[9–12] Similar NFL behavior was observed in $CaCu_3Ru_4O_{12}$ below 2 K as well.[13] In addition, NMR/NQR measurements, combined with neutron powder diffraction and electronic state calculations, argued $CaCu_3Ru_4O_{12}$ as an example of a transition-metal oxide with intermediate valence behavior.[14]

The physical origin of the enhanced effective mass of electrons in $CaCu_3Ru_4O_{12}$ is still under debate. Compared to the typical heavy fermion system, such as $CeSn_3$, Kobayashi *et al.*[5] categorized $CaCu_3Ru_4O_{12}$ as a d-electron heavy fermion system with Kondo scenario interaction between local Cu^{2+} electrons and itinerant Ru^{4+} electrons. Studies on photoelectron spectroscopy supported the Kondo scenario for the observation of a resonance-like peak at the Fermi level.[15,16] However, the evidence in NQR/NMR measurements denied the existence of a Cu localized moment,[17] and thus opposed the Kondo scenario. The investigations of the aliovalent substitution in $ACu_3Ru_4O_{12}$ (A = Na, $Na_{0.5}Ca_{0.5}$, Ca, $Ca_{0.5}La_{0.5}$) also questioned the Kondo effect as the dominant origin of

*Project supported by the National Basic Research Program of China (Grant No. 2012CB821404), the National Natural Science Foundation of China (Grant Nos. 51172166 and 61106005), the National Science Fund for Talent Training in Basic Science of China (Grant No. J1210061), and the Doctoral Fund of Ministry of Education of China (Grant No. 20110141110007).

†Corresponding author. E-mail: yongliu@whu.edu.cn

‡Corresponding author. E-mail: jshi@whu.edu.cn

© 2015 Chinese Physical Society and IOP Publishing Ltd

the effect mass enhancement. Instead, these investigations revealed the importance of the electron correlations in Ru 4d shell.[18,19]

Single crystal samples, in which the effect of grain boundaries can be eliminated, are essential in understanding the intrinsic properties of a crystalline system. Angle resolved photoemission spectroscopy (ARPES) on samples of high-quality single crystals with identified crystalline surface can offer direct information of electronic structure around the Fermi surface and provide insight of the mechanism of the enhanced effective electron mass of $CaCu_3Ru_4O_{12}$. Moreover, thermal conductivity measurements, which can be further evidence for its NFL ground state below 2 K, also require samples of high-quality single crystals. Flux-grown $CaCu_3Ru_4O_{12}$ single crystals have been synthesized by two groups of Labeau[7] and Krimmel,[13] respectively, which were mainly used to identify the crystalline structure. However, the systematical measurements of physical properties on single crystal $CaCu_3Ru_4O_{12}$ are lacking. To our best knowledge, all the measurements reported on $CaCu_3Ru_4O_{12}$ were carried out on polycrystalline samples except for the electric resistivity below 2 K.[20] In Ref. [20], the resistivity of single crystal $CaCu_3Ru_4O_{12}$ at 2 K is 1260 μΩ·cm, which is about 11 times of the resistivity of the polycrystalline sample previously reported by the same group.[13] This value is also much higher than that of the polycrystalline samples reported by other groups.[5,12] The origin of this abnormal phenomenon has not been discussed yet.

Recently, we have synthesized single crystals of $CaCu_3Ru_4O_{12}$ by flux method. The typical size of the single crystals is around $1 \times 1 \times 1$ mm^3. X-ray diffraction (XRD) and rocking curve measurements confirmed the crystals to be high quality single crystals of $CaCu_3Ru_4O_{12}$ with (100) surface. In this paper, we reported the x-ray photoelectron spectroscopy (XPS) spectra of these single crystal samples. Specific heat, magnetic susceptibility, and electric resistivity along the [100] direction of these single crystal samples are also reported.

2. Experiment

Single crystals of $CaCu_3Ru_4O_{12}$ were grown by flux method with CuO serving as flux. High-purity $CaCO_3$ (99.95%, Alfa Aesar), RuO_2 (99.95%, Alfa Aesar), and CuO (99.7%, Alfa Aesar) were used as raw materials. The mole ratio of these three kinds of oxides is 1:4:15. Raw materials were mixed thoroughly by ball milling for 12 hours, and then dried for later use. The reaction is described by

$$CaCO_3 + 3CuO + 4RuO_2 \rightarrow CaCu_3Ru_4O_{12} + CO_2\uparrow.$$

The heat treatment consists of the following processes: i) the raw materials were heated from room temperature to 1000 °C in 2 hours, then heated from 1000 °C to 1175 °C in 1 hour; ii) the samples were kept at 1175 °C for 10 hours; iii) the samples were cooled from 1175 °C to 1075 °C at a rate of 1 °C per hour; iv) the samples were cooled to room temperature without control. After that, the product was sunk in the dilute HCl (1N) solution to separate the single crystal from melted CuO. Subsequently, the single crystals were picked out, washed by distilled water, and dried. These samples were labeled by single crystal #1.

For comparison, another batch of single crystals $CaCu_3Ru_4O_{12}$ were grown by the same process stated above, but with lower purity raw materials ($CaCO_3$ (99.9%, Ruike), RuO_2 (99.5%, Ruike), and CuO (99%, Ruike)). These samples were labeled by single crystal #2. We also synthesized polycrystalline $CaCu_3Ru_4O_{12}$ by conventional solid state reaction process reported in Ref. [6].

Conventional x-ray diffraction (XRD) employing Cu Kα radiation ($\lambda = 1.54$ Å) (PhilipsX'Pert) was used to identify the crystal structure of the sample and the Miller indices of the surfaces. The measurements of x-ray rocking curve with ω scanning were performed in the (400) plane of the $CaCu_3Ru_4O_{12}$ single crystal. The x-ray single crystal data were collected with full square routine on a Bruker SMART APEXII diffractometer using Mo Kα source ($\lambda = 0.71073$ Å). X-ray photoelectron spectroscopy (XPS) measurements were carried out on a Thermo Fisher ESCALAB 250Xi instrument with a monochromatic Al Kα (1486.68 eV) x-ray source, and the samples were measured under an ultrahigh vacuum. The energy resolution was about 0.45 eV. The binding energies were calibrated using the C (1s) carbon peak (284.8 eV). All the high-resolution spectra were obtained under CAE mode with a pass energy of 20 eV and a step size of 0.05 eV.

The specific heat measurement was performed by physical properties measurement system (PPMS) commercial device (Quantum Design) from 2 K to 300 K with the relaxation method. The magnetic susceptibility along the [100] direction from 3 K to 300 K was measured using a commercial superconductor quantum interference device (SQUID, Quantum Design, PPMS). The resistivity along the [100] direction was measured by four-point probes method from 2 K to 300 K.

3. Results and discussion

Figures 1(a) and 1(b) display the pictures of one of the $CaCu_3Ru_4O_{12}$ single crystal #1 synthesized by higher purity raw materials and one of the single crystal #2 synthesized by relatively lower purity raw materials, respectively. Both of them are black crystal with a bright surface. The size of the single crystal in Fig. 1(a) is about $1 \times 1 \times 1$ mm^3, while the size of the single crystal in Fig. 1(b) is about $0.5 \times 0.5 \times 0.5$ mm^3. These are the typical size of single crystal #1 and single crystal #2, respectively.

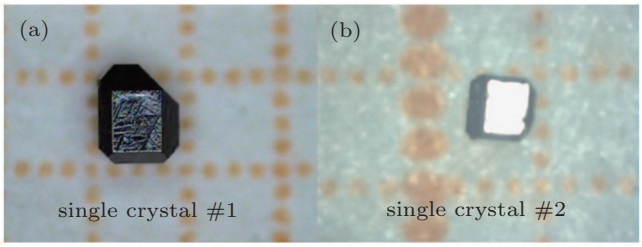


Fig. 1. (color online) $CaCu_3Ru_4O_{12}$ single crystal (each grid is 1 mm×1 mm): (a) single crystal #1, (b) single crystal #2.

As well as the difference in size, single crystals #1 and #2 also show different crystal patterns. All the surfaces of sample #1 are smooth and the edges are clear-cut. However, the surfaces of sample #2 are rough and the edges are blurry. Different crystal patterns may mainly results from different impurity concentration of raw materials according to the Kubota–Mullin model.[21]

The conventional XRD pattern of single crystal #1 is shown in Fig. 2. The sharp peaks of Bragg diffraction are indexed to be (200) and (400) plane of $CaCu_3Ru_4O_{12}$, indicating that the single crystal is well crystallized. Figures 3(a) and 3(b) show the rocking curve of (400) Brag peak of the $CaCu_3Ru_4O_{12}$ single crystal #1 and single crystal #2, respectively. The full width at half maximum of single crystal #1 is approximately 0.02 degree, while that of single crystal #2 is about 0.07 degree, indicating that the quality of the single crystal #1 synthesized by high-purity raw materials is better than that of single crystal #2 synthesized by relatively poor raw materials. Based on the data collected by single crystal x-ray diffractometer, the diffraction patterns were identified to be in the cubic space group $Im\bar{3}$ and the lattice parameter was determined to be 7.43 ± 0.009 Å, which is comparable to previously reported polycrystalline value of 7.412–7.421 Å.[17,20,22]

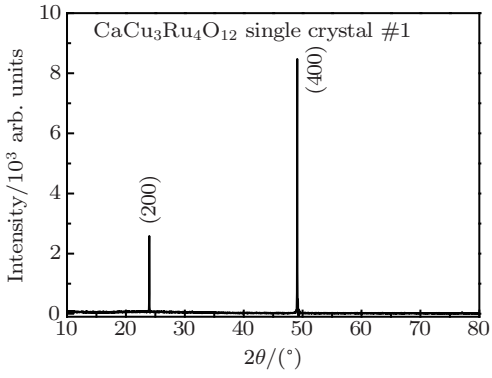


Fig. 2. X-ray diffraction patterns of $CaCu_3Ru_4O_{12}$ single crystal #1.

The XPS spectra of the single crystal #1 are given in Fig. 4. Figure 4(a) shows XPS results for Ca $2p_{3/2}$ core level with an intense peak at binding energy of 346.1 eV, which is consistent with the spectra of CaO,[23] implying that Ca ion in the sample is divalent.

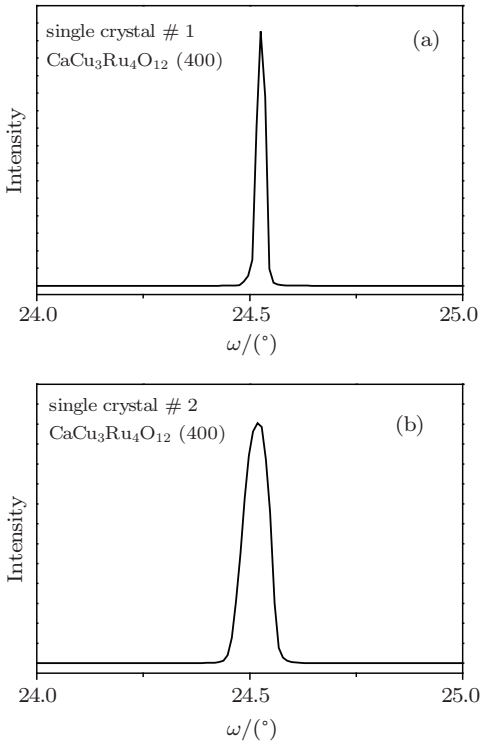


Fig. 3. (a) Rocking curve of (400) Brag peak of $CaCu_3Ru_4O_{12}$ single crystal #1. (b) Rocking curve of (400) Brag peak of $CaCu_3Ru_4O_{12}$ single crystal #2.

Figure 4(b) shows the XPS result of Cu 2p core level. It displays a satellite structure (labeled as A), a shoulder structure (labeled as B), and a well-screened structure (C). Both the position and the shape of the peaks agree with those reported in polycrystalline $CaCu_3Ru_4O_{12}$.[15] The line shape of the satellite structure is similar to those observed in CuO and La_2CuO_4, indicating the valence of Cu ions is close to +2.[15,16] The satellite structure is derived from charge transfer excitation from the O 2p orbitals to the empty Cu 3d orbitals.[15,16] In addition, the shoulder structure B and the well screened structure C arise from $d^{10}L$ (L represents an O 2p hole) and d^{10}, respectively.[15,24]

Ru 3d core level of XPS of the single crystal #1 at room temperature is shown in Fig. 4(c), which is consistent with those reported in polycrystalline $CaCu_3Ru_4O_{12}$.[15] The spectra show a double peak structure consisting of a poor-screened peak (A) at about 282.3 eV and a well-screened peak (B) at around 281.0 eV, respectively, which result from the screening of Ru 3d cores by conduction electrons.[25] The positions of the peaks are consistent with those of Ru $3d_{5/2}$ for RuO_2[26] and $SrRuO_3$,[25] which implies that the valence of Ru ions is close to +4. It is worth noting that in metallic ruthenium oxides, such as $SrRuO_3$ and $SrRu_2O_4$, the well-screened peak is dominant, but in insulating Ru oxides, such as Ca_2RuO_4, the poor-screened peak becomes dominant.[27,28] In $CaCu_3Ru_4O_{12}$ single crystal, the intensity of the well-screened peak is more dominant than those in $SrRuO_3$ and $SrRu_2O_4$, indicating that the Ru 4d electron in $CaCu_3Ru_4O_{12}$ is more itinerant compared with those in $SrRuO_3$ and $SrRu_2O_4$.

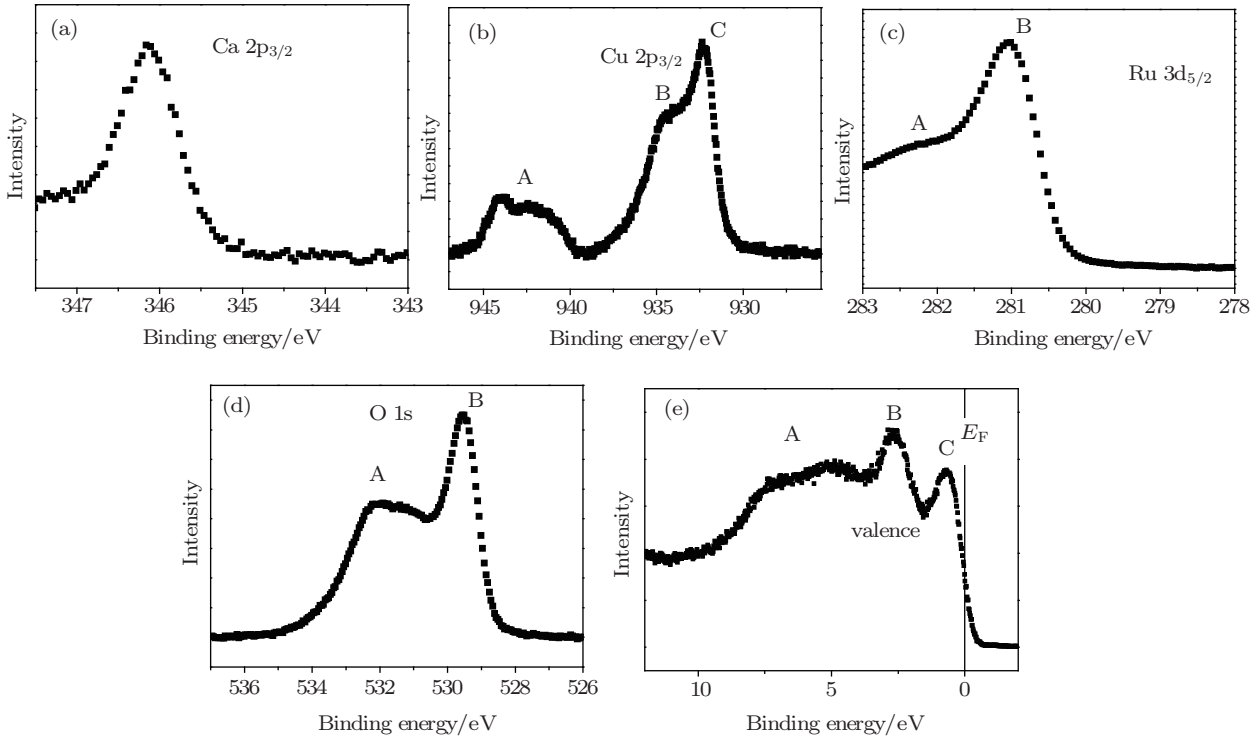


Fig. 4. (a) Ca 2p photoemission spectra of single crystal #1 taken at room temperature. (b) Cu 2p photoemission spectra of single crystal #1 taken at room temperature. (c) Ru 3d photoemission spectra of single crystal #1taken at room temperature. (d) O 1s photoemission spectra of single crystal #1 taken at room temperature. (c) Valence band of XPS spectra of single crystal #1 taken at room temperature.

As shown in Fig. 4(d), O 1s XPS spectra of $CaCu_3Ru_4O_{12}$ single crystal exhibit a strong peak at 529.6 eV and a weak peak at 532.1 eV, which associates with surface hydroxides, respectively.[29] The shape and the position of the peaks are consistent with those in CuO and RuO_2, indicating the valence state of O is -2.

Figure 4(e) shows the valence band spectra of $CaCu_3Ru_4O_{12}$ measured by XPS, which can be comparable to that of polycrystalline $CaCu_3Ru_4O_{12}$.[15,16] Three main structures can be observed, labeled as A, B, C, respectively. Based on XPS result of polycrystalline $CaCu_3Ru_4O_{12}$,[15,16] the broad structure (labeled as A) at about 5.2 eV below E_F, the peak at about 2.9 eV below E_F (labeled as B), the peak at about 0.8 eV below E_F (labeled as C), stem from the O 2p band, the Cu 3d band, the Ru $4dt_{2g}$ band, respectively. Our experimental results of valence state also agree with the calculated density of state of $CaCu_3Ru_4O_{12}$. The peaks A, B, and C correspond to the peaks A, B, and C shown in the Ref. [30].

Figure 5 illustrates the specific heat (C_P) of the $CaCu_3Ru_4O_{12}$ single crystal #1 versus T from 2 K to 300 K. As shown in the insets of Fig. 5, C_P/T shows linear dependence on T^2 below 8 K. This linear dependence can be fitted to $C_P/T = \gamma + \beta T^2$, where γ is the electron contribution and βT^2 is the phonon contribution. Our fitted γ of single crystal $CaCu_3Ru_4O_{12}$ is 90 mJ/f.u.·mol·K^2, and the fitted β results in a Debye temperature Θ_D of 280 K. For the polycrystalline $CaCu_3Ru_4O_{12}$, γ is 85 mJ/f.u.·mol·K^2, while the Debye temperature is 344 K. The γ values of both samples are 20–30 times greater than that of free electrons, revealing an enhancement of effective electron mass. It is also in good agreement with previously reported value of polycrystalline $CaCu_3Ru_4O_{12}$ (84–92 mJ/f.u.·mol·K^2)[5,13] and 83.1 mJ/f.u.·mol·K^2 calculated by first-principle method.[31] However, we note that the Debye temperature Θ_D (280 K) of the single crystal #1 is lower than 344 K of our polycrystalline sample, and far lower than 451 K and 500 K of the polycrystalline samples previously reported by Krimmel and Tanaka *et al.*[13,18]

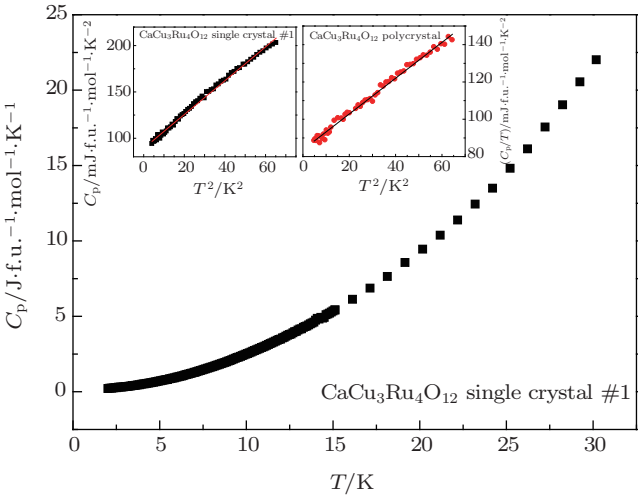


Fig. 5. (color online) Specific heat (C_P) of single crystal $CaCu_3Ru_4O_{12}$#1 versus T from 2 K to 300 K (main frame). The left and right insets show C_P/T onT^2 scale of single crystal $CaCu_3Ru_4O_{12}$ #1 and polycrystalline $CaCu_3Ru_4O_{12}$ below 8 K. The solid lines represent fitting data to $C_P/T = \gamma + \beta T^2$.

Figure 6 shows the magnetic susceptibility $\chi(T)$ of the $CaCu_3Ru_4O_{12}$ single crystal #1, single crystal #2, and polycrystal as a function of temperature from 3 K to 300 K. The strength of the external magnetic field is 1 Tesla and it is applied along the [100] direction of the single crystal samples. For the $CaCu_3Ru_4O_{12}$ single crystal #1, $\chi(T)$ is identical when H is perpendicular and parallel to [100] direction, which suggests that the magnetic ground state has a cubic symmetry.

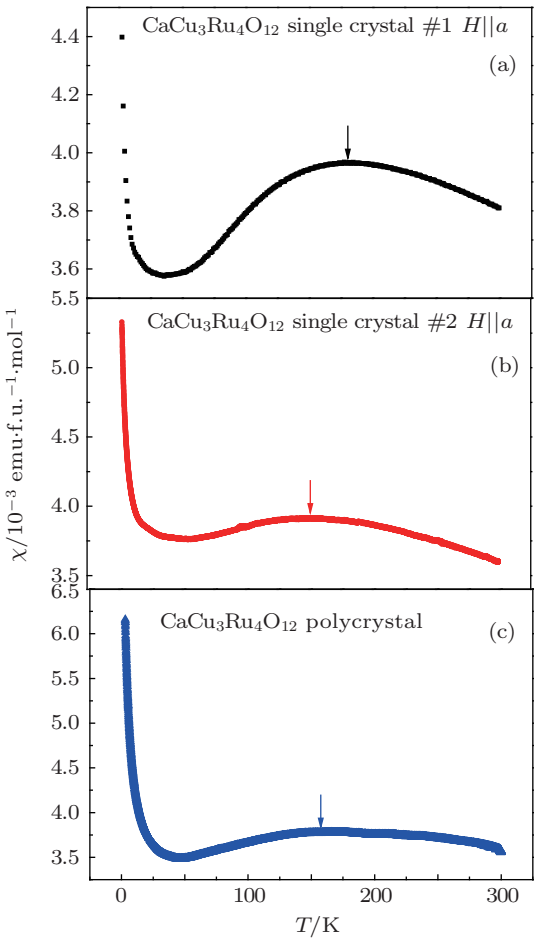


Fig. 6. (color online) (a) Temperature-dependent magnetic susceptibility of single crystal $CaCu_3Ru_4O_{12}$ #1 for $H \parallel a$ axis under $H = 1$ T. (b) Temperature-dependent magnetic susceptibility of single crystal $CaCu_3Ru_4O_{12}$ sample 2 for $H \parallel a$ axis under $H = 1$ T. (c) Temperature-dependent magnetic susceptibility of polycrystalline $CaCu_3Ru_4O_{12}$ under $H = 1$ T.

The shape of all the $\chi(T)$ in Fig. 6 agrees well with the previous reports of the $CaCu_3Ru_4O_{12}$ polycrystalline samples,[5,17] which consist of a peak and a paramagnetic tail. However, the position of the peak and the value of the paramagnetic tail at 3 K are different for different samples. The magnetic susceptibility of the polycrystal shows a broad peak around 160 K and the tail reaches 6.16 emu/f.u.·mol at 3 K. For the single crystal #2, the broad peak is about 150 K, while the tail drops to 5.32 emu/f.u.·mol at 3 K. For the single crystal #1, the peak position shifts to 180 K and the value of magnetic susceptibility decreases to 4.40 emu/f.u.·mol at 3 K. The paramagnetic tail of susceptibility of $CaCu_3Ru_4O_{12}$ at low temperature mainly results from paramagnetic impurities.[5] The smallest tail value at 3 K reveals that the single crystal #1 has the fewest paramagnetic impurities. In Kondo scenario, the broad peak is a result of the coupling between Cu^{2+} ions and Ru 4d electrons, while the position of the peak implies the strength of the coupling. Among all the samples, the peak position of the single crystal #1 occurs at the highest temperature. This indicates that the defects and/or paramagnetic impurities in $CaCu_3Ru_4O_{12}$ may weaken the coupling between Cu^{2+} ions and Ru 4d electrons.

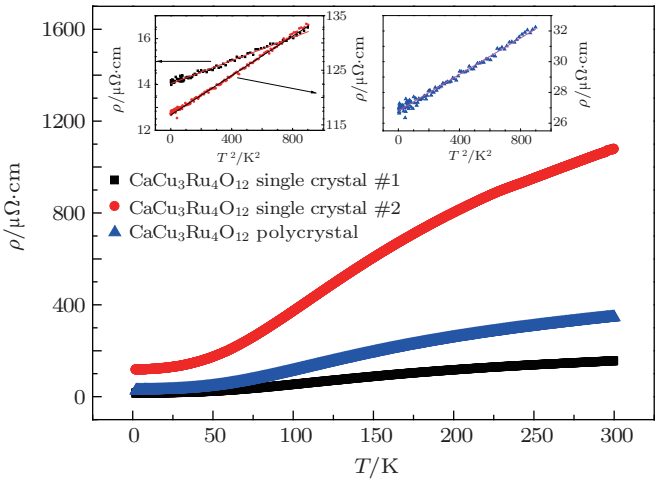


Fig. 7. (color online) Temperature-dependent resistivity of $CaCu_3Ru_4O_{12}$ single crystal #1, single crystal #2, and polycrystal from 2 K to 300 K. The electrical current is along the [100] direction for single crystal #1 and 2#. The left inset shows the resistivity of single crystal $CaCu_3Ru_4O_{12}$ #1, #2 versus T^2 below 30 K, and the right inset shows that of polycrystalline $CaCu_3Ru_4O_{12}$ versus T^2 below 30 K. The solid lines represent fitting data to $\rho = \rho_0 + AT^2$.

Figure 7 displays the electric resistivity of the $CaCu_3Ru_4O_{12}$ single crystal #1, single crystal #2, and polycrystal. The temperature range is from 2 K to 300 K and the electric current is along the [100] direction for single crystals #1 and #2. In the entire temperature range, the resistivity decreases as the temperature drops for all three samples. This further confirms that $CaCu_3Ru_4O_{12}$ is a metallic oxide. As shown in the insets of Fig. 7, below 30 K, the resistivity of all three samples satisfy the relation $\rho = \rho_0 + AT^2$, implying a typical Fermi liquid characteristic. For the single crystal sample #1, the residual resistivity ρ_0 is 14 μΩ·cm, and the coefficient A is 2.5 nΩ·cm/K^2. For the single crystal sample #2, the residual resistivity ρ_0 is 117 μΩ·cm and the coefficient A is 18 nΩ·cm/K^2. For the polycrystalline sample, the residual resistivity ρ_0 is 27 μΩ·cm and the coefficient A is 6 nΩ·cm/K^2. It is worth noting that the resistivity at all temperatures of the polycrystalline sample is greater than that of single crystal #1, but less than that of single crystal #2. Krimmer *et al.*[13,20] also found that the resistivity of single crystal samples is about 11 times that of polycrystal samples in their works. This may result from flux remnants or microcracks which exist in the

low-quality single crystal.[31] It shows that high-quality single crystal is essential in measuring the intrinsic properties of $CaCu_3Ru_4O_{12}$.

Based on the results above, the Kadowaki–Woods ratio A/γ^2 of the $CaCu_3Ru_4O_{12}$ single crystal #1 is determined to be 0.5×10^{-5} $\mu\Omega$·cm (K·mo·Ru/mJ)^2, where A is the quadratic term of the resistivity, and γ is the electron specific heat coefficient, basically satisfying the Kadowaki–Woods ratio of heavy fermion systems,[32] while the Wilson ratio is given by

$$R_{\rm W}\equiv\frac{\pi^2k_{\rm B}^2\chi\,(0)}{3\mu_{\rm B}^2\gamma(0)}\approx\frac{\pi^2k_{\rm B}^2\chi\,(3\ {\rm K})}{3\mu_{\rm B}^2\gamma(0)}=3.6,$$

where χ (3 K) is the magnetic susceptibility at 3 K and $\gamma(0)$ is the electron specific heat coefficient. This is also close to that of other heavy fermion systems. Therefore, our results of the single crystal confirm that $CaCu_3Ru_4O_{12}$ is a heavy fermion system.

4. Conclusions

High-quality single crystals $CaCu_3Ru_4O_{12}$ have been synthesized by the flux method with CuO as a flux. The size of single crystal $CaCu_3Ru_4O_{12}$ reaches $1\times1\times1$ mm^3 for the first time. The size is big enough for x-ray diffraction, which identifies the surface as (100) surface, while the rocking curve of the (400) Brag peak of the $CaCu_3Ru_4O_{12}$ single crystal shows that the full width at half maximum is approximately 0.02 degree, implying the high quality of the single crystal. In addition, the systematical measurements of properties of $CaCu_3Ru_4O_{12}$ single crystal, namely, magnetic susceptibility and electric resistivity along the [100] direction and temperature-dependent specific heat, are reported for the first time. All the results show that the single crystal and polycrystalline $CaCu_3Ru_4O_{12}$ were similar in metal-like ground state, Fermi liquid behavior between 2 K and 30 K, and enhanced effective mass of electron, which further confirms that $CaCu_3Ru_4O_{12}$ is a heavy fermion system. Other than these similarities, the single crystals have a lower Curie susceptibility tail and a smaller residual resistivity than polycrystals, which indicates that the amount of paramagnetic impurities can be controlled by tuning the number of defects in $CaCu_3Ru_4O_{12}$ samples.

References

[1] Homes C C, Vogt T, Shapiro S M, Wakimoto S and Ramirez A P 2001 *Science* **293** 673

[2] Lunkenheimer P, Fichtl R, Ebbinghaus S G and Loidl A 2004 *Phys. Rev. B* **70** 172102

[3] Zeng Z, Greenblatt M, Subramanian M A and Croft M 1999 *Phys. Rev. Lett.* **82** 3164

[4] Zeng Z, Greenblatt M, Sunstrom J E, Croft M and Khalid S 1999 *J. Solid State Chem.* **147** 185

[5] Kobayashi W, Terasaki I, Takeya J, Tsukada I and Ando Y 2004 *J. Phys. Soc. Jpn.* **73** 2373

[6] Brizé V, Autret-Lambert C, Wolfman J, Gervais M and Gervais F 2011 *J. Solid State Chem.* **184** 2719

[7] Labeau M, Bochu B, Joubert J C and Chenavas J 1980 *J. Solid State Chem.* **33** 257

[8] Subramanian M A and Sleight A W 2002 *Solid State Sci.* **4** 347

[9] Steglich F, Buschinger B, Gegenwart P, Lohmann M, Helfrich R, Langhammer C, Hellmann P, Donnevert L, Thomas S, Link A, Geibel C, Lang M, Sparn G and Assmus W 1996 *J. Phys: Condens. Matter* **8** 9909

[10] Cao G, Korneta O, Chikara S, Delong L E and Schlottmann P 2008 *Solid State Commun.* **148** 305

[11] Klein L, Antognazza L, Geballe T H, Beasley M R and Kapitulnik A 1999 *Physica B* **259** 431

[12] Petrovic C, Movshovich R, Jaime M, Pagliuso P G, Hundley M F, Sarrao J L, Fisk Z and Thompson J D 2001 *Europhys. Lett.* **53** 354

[13] Krimmel A, Günther A, Kraetschmer W, Dekinger H, Büttgen N, Eyert V, Loidl A, Sheptyakov D V, Scheidt E W and Scherer W 2008 *Phys. Rev. B* **78** 165126

[14] Krimmel A, Günther A, Kraetschmer W, Dekinger H, Büttgen N, Eyert V L A, Sheptyakov D V, Scheidt E W and Scherer W 2009 *Phys. Rev. B* **80** 121101R

[15] Tran T T, Takubo K, Mizokawa T, Kobayashi W and Terasaki I 2006 *Phys. Rev. B* **73** 193105

[16] Sudayama T, Wakisaka Y, Takubo K, Mizokawa T, Kobayashi W, Terasaki I, Tanaka S, Maeno Y, Arita M, Namatame H and Taniguchi M 2009 *Phys. Rev. B* **80** 075113

[17] Kato H, Tsuruta T, Matsumura M, Nishioka T, Sakai H, Tokunaga Y, Kambe S and Walstedt R E 2009 *J. Phys. Soc. Jpn.* **78** 054707

[18] Tanaka S, Shimazui N, Takatsu H, Yonezawa S and Maeno Y 2009 *J. Phys. Soc. Jpn.* **78** 024706

[19] Tanaka S, Takatsu H, Yonezawa S and Maeno Y 2009 *Phys. Rev. B* **80** 035113

[20] Büttgen N, Nidda H A K, Kraetschmer W, Günther A, Widmann S, Riegg S, Krimmel A and Loidl A 2010 *J. Low Temp. Phys.* **161** 148

[21] Kubota N and Mullin J W 1995 *J. Cryst. Growth* **152** 203

[22] Ebbinghaus S, Weidenkaff A and Cavaw R J 2002 *J. Solid State Chem.* **167** 126

[23] Seyama H and Soma M 1984 *J. Chem. Soc., Faraday Trans. I* **80** 237

[24] Okada K and Kotani A 2005 *J. Phys. Soc. Jpn.* **74** 653

[25] Ito A, Masumoto H and GotoT 2006 *Mater. Transact.* **47** 2808

[26] Huang C S, Houalla M, Hercules D M, Kibby C L and Petrakis L 1989 *J. Phys. Chem.* **93** 4540

[27] Cox P A, Egdell R G, Goodenough J B, Hamnett A and Naish C C 1983 *J. Phys. C* **16** 6221

[28] Sekiyama A, Kasai S, Tsunekawa M, Ishida Y, Sing M, Irizawa A, Yamasaki A, Imada S, Muro T, Saito Y, Ōnuki Y, Kimura T, Tokura Y and Suga S 2004 *Phys. Rev. B* **70** 060506(R)

[29] Poulston S, Parlett P M, Stone P and Bowker M 1996 *Surf. Interf. Anal.* **24** 811

[30] Xiang X P, Liu X J, Zhao E J, Meng J and Wu Z J 2007 *Phys. Rev. B* **76** 155103

[31] Kikugawa N, Balicas L and Mackenzie A P 2009 *J. Phys. Soc. Jpn.* **78** 014701

[32] Kadowaki K and Woods S B 1986 *Solid State Commun.* **58** 507